Crystallization of fractional charges in a strongly interacting quasihelical quantum dot

F. Cavaliere,[1,2] F. M. Gambetta,[1,2] S. Barbarino,[3] and M. Sassetti[1,2]
[1]*Dipartimento di Fisica, Università di Genova, Via Dodecaneso 33, I-16146 Genova, Italy*
[2]*SPIN-CNR, Via Dodecaneso 33, I-16146 Genova, Italy*
[3]*NEST, Scuola Normale Superiore & Istituto Nanoscienze-CNR, I-56126 Pisa, Italy*
(Received 15 September 2015; revised manuscript received 6 November 2015; published 16 December 2015)

The ground-state electron density of a one-dimensional spin-orbit coupled quantum dot with a Zeeman term and strong electron interaction is studied at the fractional helical liquid points. We show that at fractional filling factors $\nu = (2n+1)^{-1}$ (with n a non-negative integer), the density oscillates with N_0/ν peaks. For $n \geqslant 1$, a number of peaks larger than the number of electrons N_0 suggests that a *crystal of fractional charges* νe (with e the electron charge) occurs. The reported effect is amenable of verification in a dot coupled to a charged atomic force microscope tip.

DOI: 10.1103/PhysRevB.92.235128 PACS number(s): 71.10.Pm, 71.70.Ej, 71.10.Hf, 73.21.La

I. INTRODUCTION

Quasihelical electrons occur in spin-orbit coupled quantum wires when a magnetic field perpendicular to the spin-orbit field is applied [1–7]. The magnetic field opens a gap at the degeneracy point of the spin-polarized wire subbands, which is met when $k_F = k_{SO}$, with k_F the Fermi wave vector and k_{SO} the wave vector associated with the spin-orbit interaction. In this regime, and for not too strong magnetic induction, the system exhibits two helical conduction channels, with counterpropagating electrons having opposite spin polarization.

These systems, which are the subject of recent intense theoretical investigations, possess several unusual properties such as the occurrence of Majorana bound states at their edges when proximized with a superconductor [8,9] or peculiar spin oscillations in the presence of magnetic impurities [10]. The effects induced by repulsive electron interactions are remarkable: as an example, the gap induced by the magnetic field is strongly enhanced by interactions, and anisotropic spin properties occur [1,11,12].

When the Fermi level of a quasihelical wire is tuned *below* the degeneracy point, strong interactions can generate even more interesting effects. A model originally introduced to study fractional gapped phases in arrays of parallel quantum wires [13,14] treated as Luttinger liquids [15–17] has been recently applied to the four-channels Luttinger liquid describing spin-orbit coupled quantum wires [18]. The combined effects of the magnetic field and electron-electron scattering are captured by a Zeeman coupling dressed by electron interaction vertices [19]. For some critical positions of the dot Fermi level, characterized by a *fractional* filling factor with *odd* denominator

$$\nu = \frac{k_F}{k_{SO}} = \frac{1}{2n+1} \quad (n \in \mathbb{N}^*),$$

a resonance occurs, which becomes relevant in the sense of the renormalization group [18,19]. As a consequence, additional gaps open and *fractional* phases stabilize in the wire. They are accompanied by several signatures, such as the occurrence of low-energy excitations with fractional charge, which induce a noninteger quantization of the conductance [18,19]. In addition, the shot noise becomes fractionalized [20], and unusual properties of the chiral currents have been reported very recently [21].

What happens to ground-state properties, such as the electron density of a quasihelical *quantum dot*, when a fractional phase occurs? This is a nontrivial question, since it can be expected that such a peculiar state may exhibit unusual features, which would compete with the conventional Friedel [22,23] and Wigner [22,24–28] oscillations. Indeed, in any *finite-size* one-dimensional system, such as a quantum dot embedded into a quantum wire, electron density oscillations occur. A competition exists between oscillations with a $2k_F$ wave vector (Friedel oscillations), due to reflections at the dot edges, and oscillations with wave vector $4k_F$ (Wigner oscillations) due to strong electron repulsion [29]. The prevalence of either is controlled in general by the ratio between the average electron repulsion and kinetic energy. In a dot with one charge and one spin degree of freedom, Friedel oscillations have $N_0/2$ peaks (with N_0 the number of electrons in the system, assumed even for simplicity) while Wigner oscillations display N_0 peaks. In quasihelical systems, Friedel oscillations in the main gap (an integer phase with $\nu = 1$) are predicted to display N_0 peaks due to the locking between spin and momentum, which halves the number of degrees of freedom [30].

In this paper, we address this point evaluating the electron density of a quasihelical quantum dot with open boundary conditions in a fractional phase $\nu = (2n+1)^{-1}$. Along with the standard Friedel and Wigner terms and their higher harmonics [31], we consider also contributions originating from the dressed Zeeman interactions. We then evaluate the ground-state average particle density.

Our main result is that in the fractional phase $\nu = (2n+1)^{-1}$, the most relevant oscillations of the electron density have wave vector $4(2n+1)k_F$ and exhibit $(2n+1)N_0$ peaks. This is in striking contrast with the standard situation in which for strong interactions N_0 peaks occur, namely one for each electron. The presence of a *larger* number of peaks than the number of electrons suggests that this result can be interpreted as the manifestation, in the ground state, of a fractional *crystal of equally spaced charged lumps*, each peak corresponding to a νth of an electron. Charge-density oscillations can be experimentally detected, for instance in a linear transport experiment performed while scanning the dot with a charged atomic force microscope (AFM) tip [27,28,32]. We discuss

the conditions to observe this effect in state-of-the-art samples [33–35] as well as possible implementations in cold-atom systems [36,37]. A measurement of such fractional density oscillations would then constitute a probe of the fractional states.

The paper is organized as follows. In Sec. II we introduce the Luttinger model of the dot with spin-orbit coupling and magnetic field. Focusing on odd-denominator resonances, we derive an effective Hamiltonian in the strong interactions regime, and we discuss the electron density operator. In Sec. IV our results are reported and discussed in detail. Section V contains our conclusions.

II. THE MODEL

A. Zero magnetic field

We consider a one-dimensional quantum dot of length ℓ with open boundaries at $x = 0$ and $x = \ell$. The dot is subject to a spin-orbit field acting along the negative direction of the z axis. The single-particle Hamiltonian is [1,6]

$$H_{\rm sp} = -\frac{1}{2m^*}\partial_x^2 \boldsymbol{I} + i g_{\rm SO}\partial_x \boldsymbol{\sigma}_z, \tag{1}$$

where m^* is the effective electron mass, $g_{\rm SO}$ the strength of the spin-orbit coupling, with associated wave vector $k_{\rm SO} = m^* g_{\rm SO}$, and $\boldsymbol{I}$ and $\boldsymbol{\sigma}_z$ are the identity and the z Pauli matrix, respectively (here and henceforth, $\hbar = 1$).

Including forward electron-electron interactions, the Hamiltonian around the Fermi energy can be described as a two-channels Luttinger liquid

$$H_0 = \frac{1}{2\pi}\int_0^\ell dx \sum_{\mu=\rho,\sigma} v_\mu \left[\frac{1}{g_\mu}(\partial_x\phi_\mu)^2 + g_\mu(\partial_x\theta_\mu)^2\right] \tag{2}$$

with $\mu = \rho$ (σ) the charge (spin) modes and v_μ their group velocity. The parameter g_μ controls interactions and $v_\mu = v_{\rm F}/g_\mu$ in the μ sector, with $v_{\rm F}$ the Fermi velocity. For repulsive interactions one has $0 < g_\rho < 1$, while $g_\sigma = 1$ when SU(2) invariance holds. The fields $\phi_\mu(x)$ and $\theta_\mu(x)$ satisfy canonical commutation rules $[\phi_\mu(x), \partial_{x'}\theta_{\mu'}(x')] = i\pi\delta_{\mu,\mu'}\delta(x - x')$ and can be represented as

$$\phi_\mu(x) = i\sqrt{g_\mu}\sum_{n_q>0}\frac{e^{-\pi n_q\alpha/2\ell}}{\sqrt{n_q}}\sin\left(\frac{\pi n_q x}{\ell}\right)\left(b^\dagger_{\mu,n_q} - b_{\mu,n_q}\right),$$

$$\theta_\mu(x) = \frac{1}{\sqrt{g_\mu}}\sum_{n_q>0}\frac{e^{-\pi n_q\alpha/2\ell}}{\sqrt{n_q}}\cos\left(\frac{\pi n_q x}{\ell}\right)\left(b^\dagger_{\mu,n_q} + b_{\mu,n_q}\right),$$

where α is a short-length cutoff and b_{μ,n_q} are canonical bosonic operators. The fermionic operator is expressed in terms of left and right components,

$$\Psi_s(x) = e^{-isk_{\rm SO}x}[e^{ik_{\rm F}x}R_s(x) + e^{-ik_{\rm F}x}L_s(x)], \tag{3}$$

with $s = \pm$ the z direction of the electron spin. Here, $k_{\rm F} = \pi N_0/(2\ell)$ is the Fermi wave vector, with N_0 the reference number of electrons in the Fermi sea, assumed even for simplicity. The left- and right-moving fields $L_s(x)$, $R_s(x)$ satisfy $L_s(x) = -R_s(-x)$ with

$$R_s(x) = -\frac{iF_s}{\sqrt{2\pi\alpha}}e^{i\pi N_s x/\ell}e^{i\frac{\Phi_s(x)}{\sqrt{2}}}, \tag{4}$$

F_s is a Klein factor, N_s is the number of *excess* electrons in the $s = \pm$ spin sector with respect to the Fermi sea, and

$$\Phi_s(x) = \theta_\rho(x) + s\theta_\sigma(x) - \phi_\rho(x) - s\phi_\sigma(x). \tag{5}$$

Note that $[\Phi_s(x), \Phi_{s'}(-x)] = 8i\delta_{s,s'}f(x)$, with

$$f(x) = \frac{1}{2}\arctan\left[\frac{\sin\left(\frac{2\pi x}{\ell}\right)}{e^{\pi\alpha/\ell} - \cos\left(\frac{2\pi x}{\ell}\right)}\right], \tag{6}$$

due to the finite size of the dot [38].

B. Magnetic field

A magnetic field along the x axis induces a Zeeman coupling $V = \frac{1}{2}\mu_B g^* \mathcal{B}\boldsymbol{\sigma}_x \equiv \frac{B}{2}\boldsymbol{\sigma}_x$ with $\mathcal{B}$ the field intensity, μ_B the Bohr magneton, and $\boldsymbol{\sigma}_x$ the x Pauli matrix. In terms of the fermionic operators,

$$V = \frac{B}{2}\int_0^\ell dx\,[\Psi^\dagger_+(x)\Psi_-(x) + \Psi^\dagger_-(x)\Psi_+(x)]. \tag{7}$$

When $\Psi_s(x)$ is expressed via $L_s(x)$ and $R_s(x)$, eight terms arise and Eq. (7) becomes

$$V = \frac{1}{2\pi}\sum_{j=1}^{8}\int_0^\ell dx\, V_j(x)\,. \tag{8}$$

In the presence of electron interactions, the Zeeman coupling induces also scattering processes in which each term $V_j(x)$ is *dressed* by backscattering interaction vertices [18,19] $U_n(x) = [e^{2ik_{\rm F}x}L^\dagger_\pm(x)R_\pm(x)]^n$, with n a non-negative integer. They can be represented as [39]

$$V_j(x) \to V_j^{(n)}(x) = U_n(x)V_j(x)U_n(x), \tag{9}$$

with the corresponding Hamiltonian

$$V = \frac{1}{2\pi}\sum_{n\geqslant 0}\sum_{j=1}^{8}\int_0^\ell dx\, V_j^{(n)}(x). \tag{10}$$

In bosonic form,

$$V_j^{(n)}(x) = \Delta_j^{(n)}\cos\left[2q_j^{(n)}x - \sqrt{2}O_j^{(n)}(x)\right], \tag{11}$$

where $\Delta_j^{(n)}$ are interaction amplitudes $\propto B$.

The operators $O_j^{(n)}(x)$ and wave vectors $q_j^{(n)}$ are presented in Table I, where $\gamma_n = 2n + 1$. We have omitted zero modes describing excess electrons beyond the Fermi sea, which are irrelevant for the forthcoming discussions focusing on the behavior at the Fermi surface with N_0 electrons. Note that $O_3^{(n+1)}(x) = O_4^{(n)}(x)$, $q_3^{(n+1)}(x) = q_4^{(n)}(x)$, so that terms $V_3^{(n+1)}(x)$ and $V_4^{(n)}(x)$ could be regrouped, with the exception of the term $V_3^{(0)}(x)$.

The first four terms [40], $1 \leqslant j \leqslant 4$, oscillate with a wavelength shorter than ℓ and therefore give negligible contributions to the Hamiltonian in the sense of the renormalization group [18,19].

On the other hand, by suitably tuning $k_{\rm SO}$ and $k_{\rm F}$, terms with $5 \leqslant j \leqslant 8$ can become spatially nonoscillating and thus resonant. In particular, if $k_{\rm F} = k_{\rm SO}/(2n)$ ($n \geqslant 1$), the terms $V_5^{(n)}(x)$ and $V_6^{(n)}(x)$ become resonant, while for $k_{\rm F} = k_{\rm SO}/(2n + 1)$

TABLE I. Bosonized expression of the eight Zeeman terms dressed by electron-electron interactions and their corresponding wave vector. Here, $\gamma_n = 2n+1$ and $F_0^{(n)}(x) = 2\sqrt{2}(1-\gamma_n)f(x)$.

j	$O_j^{(n)}(x)$	$q_j^{(n)}$
1	$(\gamma_n-1)\phi_\rho(x)+\theta_\sigma(x)-\phi_\sigma(x)$	$(\gamma_n-1)k_F+k_{SO}$
2	$(\gamma_n-1)\phi_\rho(x)+\theta_\sigma(x)+\phi_\sigma(x)$	$(\gamma_n-1)k_F+k_{SO}$
3	$(\gamma_n-2)\phi_\rho(x)+\theta_\sigma(x)$	$(\gamma_n-2)k_F+k_{SO}$
4	$\gamma_n\phi_\rho(x)+\theta_\sigma(x)$	$\gamma_n k_F+k_{SO}$
5	$(\gamma_n-1)\phi_\rho(x)-\theta_\sigma(x)+\phi_\sigma(x)-F_0^{(n)}(x)$	$(\gamma_n-1)k_F-k_{SO}$
6	$(\gamma_n-1)\phi_\rho(x)-\theta_\sigma(x)-\phi_\sigma(x)-F_0^{(n)}(x)$	$(\gamma_n-1)k_F-k_{SO}$
7	$\gamma_n\phi_\rho(x)-\theta_\sigma(x)-F_0^{(n)}(x)$	$\gamma_n k_F-k_{SO}$
8	$(\gamma_n-2)\phi_\rho(x)-\theta_\sigma(x)-F_0^{(n)}(x)$	$(\gamma_n-2)k_F-k_{SO}$

($n \geqslant 0$), the terms $V_7^{(n)}(x)$ and $V_8^{(n+1)}(x)$ resonate. Terms with $j=5,6$ ($j=7,8$) are predicted to give rise to *fractional* states in the dot [13,14,18,19] with filling factor $\nu = 1/(2n)$ [$\nu = 1/(2n+1)$].

The above resonance conditions can be rewritten in terms of the average density $n_0 = N_0/\ell$ as

$$n_0 = \frac{2m^* g_{SO}}{\pi\hbar^2}\nu, \tag{12}$$

where we have reinserted $\hbar$ for clarity. For a resonance with a given ν, the right-hand side of Eq. (12) is fixed by the material parameters. By tuning the average particle density via N_0 and ℓ, the dot can be brought into resonance. Note that, due to the finite dot length, k_F is quantized so that for a given n and number of electrons N_0 only certain values of k_{SO} satisfy the resonance condition—see also Sec. IV B.

In the following, we will consider only *odd denominator* resonances [41], i.e., those at $k_F = k_{SO}/(2n+1)$. Once resonating, the terms $V_7^{(n)}(x)$ and $V_8^{(n+1)}(x)$ become relevant in the spirit of the renormalization group [18,19] when $g_\rho \ll g_c$ with $g_c = 3/(2n+1)^2$. Thus, for sufficiently strong interactions one can retain only the dominant terms of Eq. (10):

$$\begin{aligned} V &\approx \frac{1}{2\pi}\int_0^\ell dx\big[V_7^{(n)}(x)+V_8^{(n+1)}(x)\big] \\ &= \frac{\Delta}{2\pi}\int_0^\ell dx\cos[4f(x)]\cos[2\eta_+(x)], \end{aligned} \tag{13}$$

where $\Delta_7^{(n)} = \Delta_8^{(n+1)} = \Delta/2$, and we have performed the canonical transformation

$$\eta_+(x) = \tfrac{1}{\sqrt{2}}[\gamma_n\phi_\rho(x)-\theta_\sigma(x)] + 2\gamma_n f(x), \tag{14a}$$

$$\eta_-(x) = \tfrac{1}{\sqrt{2}}[\gamma_n\phi_\rho(x)+\theta_\sigma(x)], \tag{14b}$$

$$\chi_\pm(x) = \tfrac{1}{\sqrt{2}}\big[\gamma_n^{-1}\theta_\rho(x) \mp \phi_\sigma(x)\big], \tag{14c}$$

with $\eta_\pm(x)$ and $\chi_\pm(x)$ canonically conjugated fields.

The Hamiltonian $H = H_0 + V$ can then be decoupled into a massless and a massive term, $H \approx h_0 + h_M$, where

$$h_0 = \frac{v_\eta}{2\pi}\int_0^\ell dx\left[\frac{1}{g_\eta}(\partial_x\eta_-)^2 + g_\eta(\partial_x\chi_-)^2\right], \tag{15}$$

$$\begin{aligned} h_M = {} & \frac{v_\eta}{2\pi}\int_0^\ell dx\left[\frac{1}{g_\eta}(\partial_x\eta_+)^2 + g_\eta(\partial_x\chi_+)^2\right] \\ & + \frac{\Delta}{2\pi}\int_0^\ell dx\cos[4f(x)]\cos[2\eta_+(x)], \end{aligned} \tag{16}$$

with

$$v_\eta = \frac{1+\gamma_n^2}{2}\frac{v_F}{g_\eta}, \quad g_\eta = \gamma_n\sqrt{\frac{1+\gamma_n^2}{1+\gamma_n^2 g_\rho^2}}\, g_\rho. \tag{17}$$

The massless sector is a standard Luttinger liquid [15–17] with renormalized parameters v_η and g_η, while the massive term is a sine-Gordon model. Note that identifying $H \approx h_0 + h_M$ neglects corrections $U_\eta \propto (\partial_x\eta_+)(\partial_x\eta_-)$ and $U_\chi \propto (\partial_x\chi_+)(\partial_x\chi_-)$. A mean-field analysis of these terms [1] reveals that the term U_η is subleading since the field $\eta_+(x)$ is essentially pinned to one of the minima of the sine-Gordon term in the regime treated in this paper (see below). The term U_χ is more easily treated in the action formalism, where a similar analysis shows that it leads to corrections leading to a renormalization [1] of v_η^* and g_η^*.

The dynamics of the massless sector is standard. Concerning the massive sector with a sine-Gordon term, the equation of motion for $\eta_+(x)$ is

$$\frac{v_\eta}{g_\eta}\partial_x^2\eta_+(x) + \Delta\cos[4f(x)]\sin[2\eta_+(x)] = 0. \tag{18}$$

In the scaling limit $g_\rho \ll g_c$ that we consider, Δ diverges under renormalization-group transformations [18,19], and the *semiclassical* solutions for the equation of motion "pin" the field $\eta_+(x)$ to the minima of the cosine term, i.e.,

$$\eta_+(x) = \frac{\pi}{2} + k\pi \qquad (k \in \mathbb{Z}), \tag{19}$$

with the conjugated field $\chi_+(x)$ becoming a strongly fluctuating one: $\langle\chi_+^2(x)\rangle \to \infty$, where $\langle\cdots\rangle$ represents the quantum average over the ground state. This is the infinite mass limit of the model [18,19].

When the field $\eta_+(x)$ is pinned as in Eq. (19), a gap in the spectrum opens. For $n=0$ ($\nu=1$), Eq. (13) is relevant for $g_\rho \leqslant 3$ and corresponds to the opening of a gap near the degeneracy point of the spin-polarized wire subbands. This constitutes the *main gap* of the theory, which requires no repulsive interaction among electrons to be formed, where a quasihelical electron liquid develops [1–6].

More intriguing are the properties of the *fractional* gaps occurring for $n \geqslant 1$ at fractional fillings,

$$\nu = \frac{1}{2n+1}.$$

These gaps do not appear in a noninteracting theory and will be the ones addressed in the rest of the paper.

C. Electron density operator

To study the properties of the ground-state particle density, we start by observing that the density operator $\rho(x)$ is

composed of several terms [22,23,31,38,42–44],

$$\rho(x) = \rho_{\rm LW}(x) + \lambda_{\rm F}\rho_{\rm F}(x) + \lambda_{\rm W}\rho_{\rm W}(x) + \lambda_{\rm Z}\rho_{\rm Z}(x), \quad (20)$$

with the weights λ_i ($i \in \{\rm F,W,Z\}$) free parameters to be determined imposing suitable constraints on $\rho(x)$, namely open boundary conditions and the conservation of the number of electrons.

Here,

$$\rho_{\rm LW}(x) = \frac{N_0}{\ell} + \frac{1}{\pi}\partial_x\phi_\rho(x) \quad (21)$$

is the long-wave part of the density.

The contribution of the Friedel oscillations [22,23,45] is

$$\rho_{\rm F}(x) = \sum_{m=1}^{\infty} \rho_{\rm F}^{(m)}(x) \quad (22)$$

with

$$\rho_{\rm F}^{(m)}(x) = \cos\{2m[k_{\rm F}x - f(x)] - \sqrt{2}m\phi_\rho(x)\} \times \cos[\sqrt{2}m\phi_\sigma(x)] \quad (23)$$

the Friedel harmonics at wave vector $2mk_{\rm F}$ ($m \geqslant 1$).

Interactions and umklapp scattering induce Wigner oscillations [31,38,42–44]

$$\rho_{\rm W}(x) = \sum_{m=1}^{\infty} \rho_{\rm W}^{(m)}(x), \quad (24)$$

with harmonics

$$\rho_{\rm W}^{(m)}(x) = \cos\{4m[k_{\rm F}x - f(x)] - 2\sqrt{2}m\phi_\rho(x)\} \quad (25)$$

at wave vector $4mk_{\rm F}x$.

Finally, a contribution induced by all terms in Eq. (10) that do not become resonant,

$$\rho_{\rm Z}(x) = \sum_{m=1}^{\infty}\sum_{j=1}^{8}[1 - (\delta_{m,n}\delta_{j,7} + \delta_{m,n+1}\delta_{j,8})]\rho_{{\rm Z},j}^{(m)}, \quad (26)$$

with

$$\rho_{{\rm Z},j}^{(m)}(x) = \cos\left[2q_j^{(m)}x - \sqrt{2}O_j^{(m)}(x)\right], \quad (27)$$

is considered.

The terms in Eqs. (24) and (26)—and the higher harmonics of the Friedel oscillations—are introduced here as corrections to the usual density operator in a Luttinger liquid quantum dot. They are introduced to capture the effects of nonresonant terms that are not directly included in the Hamiltonian $h_0 + h_M$—see Eqs. (15) and (16). To motivate them, we consider explicitly the case of terms $V_j^{(m)}(x)$—a similar argument holds for the Wigner terms. To the lowest perturbative order, such terms induce a perturbation $\langle\delta\rho_{{\rm LW},j}^{(m)}(x)\rangle$ to the long-wave term [44],

$$\langle\delta\rho_{{\rm LW},j}^{(m)}(x)\rangle \propto \int_0^\ell dy \sum_{\mathcal{E}} \frac{\langle\mathcal{E}|V_j^{(m)}(y)|\mathbf{0}\rangle\langle\mathbf{0}|\partial_x\phi_\rho(x)|\mathcal{E}\rangle}{E_{\mathbf{0}} - E_{\mathcal{E}}},$$

where $|\mathcal{E}\rangle$ represents a many-body excitation of the unperturbed dot with ground state $|\mathbf{0}\rangle$, and $E_{\mathcal{E}}$ is the corresponding unperturbed energy. Note that terms with $j = 7$, $m = n$ and $j = 8$, $m = n + 1$ must not be considered here, since they are explicitly included in the Hamiltonian. As shown in detail in Appendix A, this correction has the form

$$\langle\delta\rho_{{\rm LW},j}^{(m)}(x)\rangle \propto \frac{\cos\left[2q_j^{(m)}x + C_j^{(m)}f(x)\right]}{q_j^{(m)}}, \quad (28)$$

with $C_j^{(m)}$ a scalar coefficient, and thus it oscillates with wave vector $q_j^{(m)}$. These oscillating corrections are enveloped by slowly varying terms that scale as a power law with the Luttinger parameters of the massless sector. On the other hand, as shown in Sec. III, the quantum average of the terms $\rho_{{\rm Z},j}^{(m)}(x)$ produces in the particle density the same kind of oscillations of Eq. (28), with the same slowly varying envelope function.

One can therefore capture the effects of interactions not considered by the effective Hamiltonian $h_0 + h_M$ by including the extra terms $\rho_{{\rm Z},j}^{(m)}(x)$ in the particle density operator. A similar argument motivates the inclusion of $\rho_{\rm W}^{(m)}(x)$ [44].

III. QUANTUM AVERAGE OF THE ELECTRON DENSITY

Let us now turn to the evaluation of the quantum average of the electron density $\rho(x)$—see Eq. (20)—on the ground state in the fractional gapped phase.

The long-wave term $\rho_{\rm LW}(x)$ in Eq. (21) simply evaluates N_0/ℓ. Each of the other terms—see Eqs. (22), (24), and (26)—can be cast into the form

$$O = \cos\left[Q(x) + \sum_{p=\pm}[\alpha_p\eta_p(x) + \beta_p\chi_p(x)]\right], \quad (29)$$

where $Q(x) = qx + c_Q f(x)$, with q the wave vector of the oscillating term and c_Q a scalar coefficient. Note that for the dressed Zeeman terms, the wave vector is $q = 2q_j^{(m)}$—see Eq. (27)—while for the Wigner terms the wave vector is $q = 4mk_F$—see Eq. (25). To evaluate the averages, we convert in the product form

$$O = e^{iQ'(x)}\prod_{p=\pm} e^{i\alpha_p\eta_p(x)}\prod_{p=\pm} e^{i\beta_p\chi_p(x)} + \text{H.c.}, \quad (30)$$

where

$$Q'(x) = Q(x) - \alpha_-\beta_+ f(x) \quad (31)$$

also includes the effects of commutations between fields.

Let us first consider the massive sector $p = +$. In the scaling limit of very large mass, $\eta_+(x)$ is pinned to the minima of the sine-Gordon potential; see Eq. (19). All these minima are degenerate, with the jth minimum having energy $\varepsilon_j = -|\varepsilon_0|\ \forall\ j$, with

$$\varepsilon_0 = -\frac{\Delta}{2\pi}\int_0^\ell dx\cos[4f(x)]. \quad (32)$$

The average of $\exp[i\alpha_+\eta_+(x)]$ is then

$$\langle e^{i\alpha_+\eta_+(x)}\rangle = e^{i\varphi_0}\lim_{J\to\infty}\sum_{j=-J}^{J}\frac{e^{-\beta\varepsilon_j}e^{i\pi\alpha_+ j}}{\mathcal{Z}_J}, \quad (33)$$

where $\varphi_0 = \pi\alpha_+/2$ and $\mathcal{Z}_J = \sum_{j=-J}^{J} e^{-\beta\varepsilon_j}$ with a fictitious small temperature $\propto\beta^{-1}$, which can be set to zero in the end of the calculation. If $\alpha_+ = 2l$, with $l \in \mathbb{Z}$, the above expression

reduces to $(-1)^l$. If $\alpha_+ \neq 2l$, however, the partial summations cancel out and the average is zero. Thus we conclude that

$$\langle e^{i\alpha_+\eta_+(x)}\rangle = (-1)^l \delta_{\alpha_+,2l} \quad (l \in \mathbb{Z}). \tag{34}$$

Note that this sharp condition is due to the degeneracy of the minima of the potential (see Sec. IV B).

Furthermore, we have

$$\langle e^{i\beta_+\chi_+(x)}\rangle = [E(x)]^{\frac{\beta_+^2}{2}}, \tag{35}$$

where

$$E(x) = e^{-\langle\chi_+^2(x)\rangle} \to 0 \tag{36}$$

due to the large fluctuations of the field $\chi_+(x)$. Thus, every operator that contains the field $\chi_+(x)$ will be vanishing in the infinite mass limit.

In the massless sector, the (zero-temperature) averages $\langle\eta_-^2(x)\rangle$ and $\langle\chi_-^2(x)\rangle$ can be evaluated from the correlators [46]

$$\mathcal{G}(x,x';\tau) = \langle T_\tau \eta_-(x,\tau)\eta_-(x',0)\rangle, \tag{37}$$

$$\bar{\mathcal{G}}(x,x';\tau) = \langle T_\tau \chi_-(x,\tau)\chi_-(x',0)\rangle, \tag{38}$$

where τ is the imaginary time, as

$$\langle\eta_-^2(x)\rangle = \lim_{\tau\to\alpha/\pi v_\eta} \mathcal{G}(x,x;\tau), \tag{39}$$

$$\langle\chi_-^2(x)\rangle = \lim_{\tau\to\alpha/\pi v_\eta} \bar{\mathcal{G}}(x,x;\tau), \tag{40}$$

with $\alpha(\pi v_\eta)^{-1}$ a short imaginary-time cutoff. Let us focus on $\mathcal{G}(x,x';\tau)$, as the procedure is analogous for $\bar{G}(x,x';\tau)$. Introducing the Fourier transform

$$\mathcal{G}_\omega(x,x') = \int_0^\beta \frac{d\tau}{2\pi}\, \mathcal{G}(x,x';\tau)e^{-i\omega\tau} \tag{41}$$

from the Hamiltonian in Eq. (15), one has

$$\left[-\frac{2v_\eta}{g_\eta}\partial_x^2 + \frac{2\omega^2}{v_\eta g_\eta}\right]\mathcal{G}_\omega(x,x') = \delta(x-x'). \tag{42}$$

Imposing $\eta_-(-x) = -\eta_-(x)$ and $\eta_-(x+2\ell) = \eta_-(x)$ as appropriate for open-boundary conditions, one finds

$$\mathcal{G}_\omega(x,x') = \frac{v_\eta g_\eta}{\ell}\sum_{j=1}^{\infty}\frac{\sin(k_j x)\sin(k_j x')}{\omega^2 + v_\eta^2 k_j^2}, \tag{43}$$

with $k_j = (\pi/\ell)j$. Thus, we get

$$\langle\eta_-^2(x)\rangle = -\frac{g_\eta}{2}\log[K(x)], \tag{44}$$

where

$$K(x) = \frac{\sinh\left(\frac{\pi\alpha}{2\ell}\right)}{\sqrt{\sinh^2\left(\frac{\pi\alpha}{2\ell}\right) + \sin^2\left(\frac{\pi x}{\ell}\right)}}. \tag{45}$$

Similarly, one finds

$$\langle\chi_-^2(x)\rangle = -\frac{1}{2g_\eta}\log[G(x)], \tag{46}$$

TABLE II. Coefficients for the different contributions to the electron density.

Term	α_+	α_-	β_+	β_-	Wave vector
$\rho_F^{(m)}(x)$	$-\frac{m}{\gamma_n}$	$-\frac{m}{\gamma_n}$	1	-1	$2mk_F$
$\rho_W^{(m)}(x)$	$-2\frac{m}{\gamma_n}$	$-2\frac{m}{\gamma_n}$	0	0	$4mk_F$
$\rho_{Z,1}^{(m)}(x)$	$\frac{\gamma_n-\gamma_m+1}{\gamma_n}$	$\frac{1-\gamma_m-\gamma_n}{\gamma_n}$	-1	1	$2(\gamma_m+\gamma_n-1)k_F$
$\rho_{Z,2}^{(m)}(x)$	$\frac{\gamma_n-\gamma_m+1}{\gamma_n}$	$\frac{1-\gamma_m-\gamma_n}{\gamma_n}$	1	-1	$2(\gamma_m+\gamma_n-1)k_F$
$\rho_{Z,3}^{(m)}(x)$	$\frac{\gamma_n-\gamma_{m-1}}{\gamma_n}$	$-\frac{\gamma_n+\gamma_{m-1}}{\gamma_n}$	0	0	$2(\gamma_{m-1}+\gamma_n)k_F$
$\rho_{Z,4}^{(m)}(x)$	$\frac{\gamma_n-\gamma_m}{\gamma_n}$	$-\frac{\gamma_n+\gamma_m}{\gamma_n}$	0	0	$2(\gamma_m+\gamma_n)k_F$
$\rho_{Z,5}^{(m)}(x)$	$\frac{1-\gamma_n-\gamma_m}{\gamma_n}$	$\frac{1-\gamma_m+\gamma_n}{\gamma_n}$	-1	1	$2(\gamma_m-\gamma_n-1)k_F$
$\rho_{Z,6}^{(m)}(x)$	$\frac{1-\gamma_n-\gamma_m}{\gamma_n}$	$\frac{1-\gamma_m+\gamma_n}{\gamma_n}$	1	-1	$2(\gamma_m-\gamma_n-1)k_F$
$\rho_{Z,7}^{(m)}(x)$	$-\frac{\gamma_n+\gamma_m}{\gamma_n}$	$\frac{\gamma_n-\gamma_m}{\gamma_n}$	0	0	$2(\gamma_m-\gamma_n)k_F$
$\rho_{Z,8}^{(m)}(x)$	$-\frac{\gamma_n+\gamma_{m-1}}{\gamma_n}$	$\frac{\gamma_n-\gamma_{m-1}}{\gamma_n}$	0	0	$2(\gamma_{m-1}-\gamma_n)k_F$

with

$$G(x) = 4e^{-\frac{\pi\alpha}{\ell}}\sinh^2\left(\frac{\pi\alpha}{2\ell}\right)\cosh\left(\frac{\pi\alpha}{2\ell}\right)K^{-1}(x). \tag{47}$$

Thus in the massless sector one has

$$\exp\left[-\frac{\alpha_-^2}{2}\langle\eta_-^2(x)\rangle\right] = [K(x)]^{\alpha_-^2 g_\eta/4}, \tag{48}$$

$$\exp\left[-\frac{\beta_-^2}{2}\langle\chi_-^2(x)\rangle\right] = [G(x)]^{\beta_-^2/(4g_\eta)}. \tag{49}$$

Summarizing, one obtains for the operator in Eq. (30)

$$\langle O\rangle = \sum_l (-1)^l \delta_{\alpha_+,2l}[K(x)]^{\frac{\alpha_-^2 g_\eta}{4}}[G(x)]^{\frac{\beta_-^2}{4g_\eta}} \times [E(x)]^{\frac{\beta_+^2}{2}}\cos[Q'(x)]. \tag{50}$$

The scaling limit imposes severe restrictions to Eq. (50), due to the simultaneous requirements $\alpha_+ = 2l$ and $\beta_+ = 0$, with l an integer.

Table II shows the coefficients and the wave vector for the different oscillating components of the electron density in Eq. (20). It can be seen that $\rho_F^{(m)}(x) = \rho_{Z,1}^{(m)}(x) = \rho_{Z,2}^{(m)}(x) = \rho_{Z,5}^{(m)}(x) = \rho_{Z,6}^{(m)}(x) = 0$ due to the exponential suppression induced by the large fluctuations of $\chi_+(x)$.

The Wigner harmonics only survive if $m = l\gamma_n$ (with $l \in \mathbb{Z}^*$), see Table II and Eq. (34), and they have wave vector $l4\gamma_n k_F$. They scale as $[K(x)]^{l^2 g_\eta}$. Among them, the most relevant term corresponds to $l = 1$, with wave vector $Q_0 = 4\gamma_n k_F$.

Going through Table II, one verifies that similar arguments apply for every nonvanishing oscillating term $\rho_{Z,j}^{(m)}(x)$: they all have the wave vector of the form $l4\gamma_n k_F$ (with $l \in \mathbb{Z}^*$) and scale as $[K(x)]^{l^2 g_\eta}$. Thus, we can conclude that the only contributions to the electron density oscillate with wave vectors $l4\gamma_n k_F$.

Among these terms, the most relevant ones have wave vector $Q_0 = 4\gamma_n k_F$ and scale as $[K(x)]^{g_\eta}$. When all the most relevant terms are collected and physical constraints (open boundary conditions and normalization) are imposed on $\langle\rho(x)\rangle$

to determine λ_W and λ_Z, we obtain

$$\langle\rho(x)\rangle = \frac{N_0}{\ell}\left\{1 - \frac{[K(x)]^{g_\eta}}{5}\sum_{i=1}^{5}\cos\left[Q_0 x - F_i(x)\right]\right\}, \quad (51)$$

where $F_1(x) = F_2(x) = F_3(x) = 0$, $F_4(x) = 4(\gamma_n - 1)f(x)$, and $F_5(x) = 4(\gamma_n + 1)f(x)$. The terms $F_{4,5}(x) \propto f(x)$ are a direct consequence of the dot finite size [38] and stem from the terms $\rho^{(m)}_{Z,7}(x)$ and $\rho^{(m)}_{Z,8}(x)$, respectively.

IV. RESULTS

A. Density oscillations and fractional charges

Let us now turn to a discussion of the results. In the main gap $n = 0$ (with $\gamma_n = 1$), the only nonvanishing contributions to $\rho(x)$ are the lowest Wigner harmonic $\rho^{(1)}_W(x)$—see Eq. (25)—and four terms stemming from $\rho_Z(x)$. They all have wave vector $4k_F$. The density displays N_0 oscillations corresponding to the expected Wigner oscillations of N_0 electrons in a box [22,24,30]. For $n \geqslant 1$, however, the density exhibits $(2n + 1)N_0$ peaks. This is due to the contribution of the relevant nonzero terms in $\rho_Z(x)$ and of the $(2n + 1)$th Wigner harmonic.

Figures 1 and 2 show $\langle\rho(x)\rangle$ for $N_0 = 6$ and 10 particles, respectively, in the case of the lowest resonances $n = 0$, 1, and 2. As can be seen, the density shows the expected number of peaks, $N_p = (2n + 1)N_0$. For $n \geqslant 1$, a density displaying $N_p > N_0$ peaks is a fascinating situation in which the many-body wave function of the N_0 electrons splits up. This splitting can be suggestively interpreted as the crystallization of $(2n + 1)N_0$ "agglomerates," each with a charge $ve = e/(2n + 1)$, which distribute evenly in space minimizing the strong repulsive interactions among them. This would give rise to N_p distinct peaks in the density.

It is very interesting to observe that, although several predictions have already been made concerning fractional *excitations* in strongly interacting spin-orbit coupled wires in the presence of a magnetic field [18–21], in this work we predict that a bulk ground-state property—the density $\rho(x)$—exhibits signatures very similar to such entities.

In this context, very recently a similar phenomenon was reported in which the density of strongly interacting edge states of a two-dimensional topological insulator with two-particle backscattering exhibits $2N_0$ peaks for N_0 electrons, and it was attributed to the formation of a "fractional Wigner crystal" [47].

Signatures of fractional charged lumps also show up in higher-order functions, such as the density-density correlation functions [30]. Indeed, preliminary results (not shown) confirm that these correlators display $N_p - 1$ oscillations, seeming to imply a degree of correlations among the fractional density peaks. This would point toward their description in terms of fractional quasiparticles. Work to confirm this interpretation is currently underway.

From Figs. 1 and 2 it is possible to notice the appearance of a slowly varying modulation superimposed to the peaks, induced by the terms $f(x)$ present in $F_{4,5}(x)$ of Eq. (51) arising from the open-boundary conditions. Such terms are responsible, in the case of a standard Wigner molecule, of a weak distortion that tends to "squeeze" the outermost electrons toward the center [38]. In the present case, the slowly varying modulation of the density is induced by the superposition of slightly distorted oscillations, ultimately producing a weak beatinglike pattern. Finally, one should also note that an envelope due to $[K(x)]^{g_\eta}$ is present, but its effect is negligible in the strong interaction regime presented here.

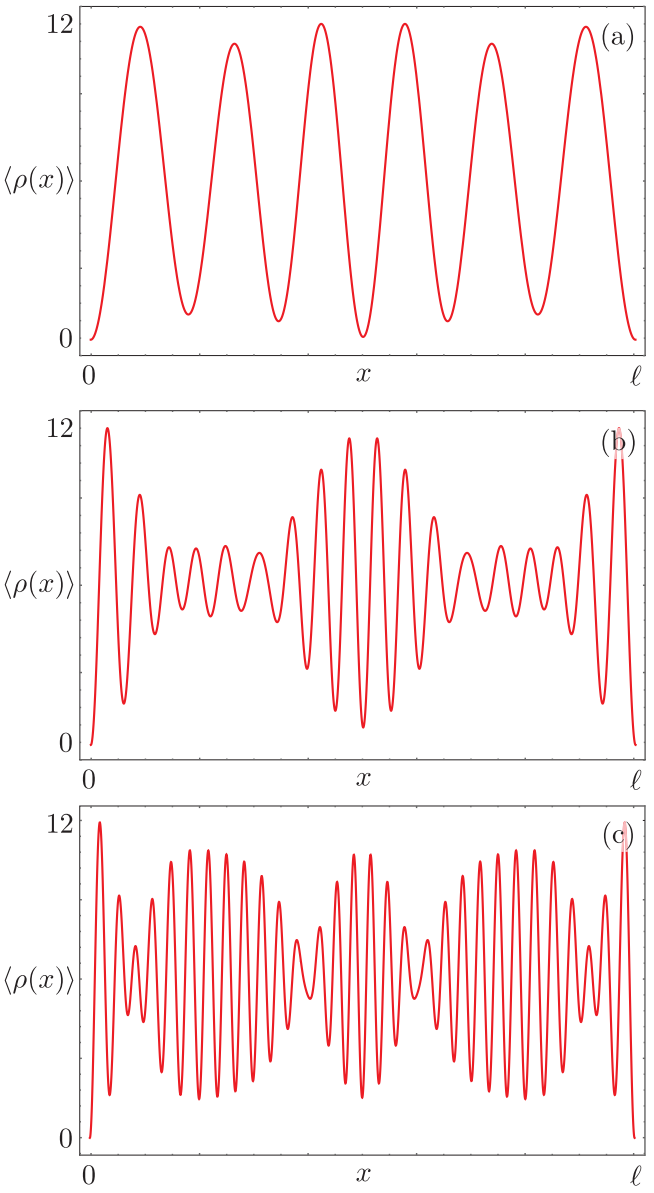

FIG. 1. (Color online) Plot of the $\rho(x)$ (units ℓ^{-1}) for a dot with $N_0 = 6$ electrons and $g_\rho = 0.05$ at the resonance (a) $n = 0$, (b) $n = 1$, and (c) $n = 2$. In all panels, $\alpha = k_F^{-1}$.

In deriving Eq. (51), all the nonzero dressed Zeeman terms $\rho^{(m)}_{Z,j}(x)$ have been weighted with the same factor λ_Z. However, since all the relevant terms have the same wave vector, we expect that the number of oscillations of the density is robust, with only a possibly different modulation pattern of the peaks due to different weights of terms with $F_4(x)$ and $F_5(x)$. It may also be speculated that within the fractional phase, Wigner oscillations have a weaker amplitude than the term $\rho_Z(x)$. In this case we also conclude, in analogy to what was discussed previously, that our results are robust.

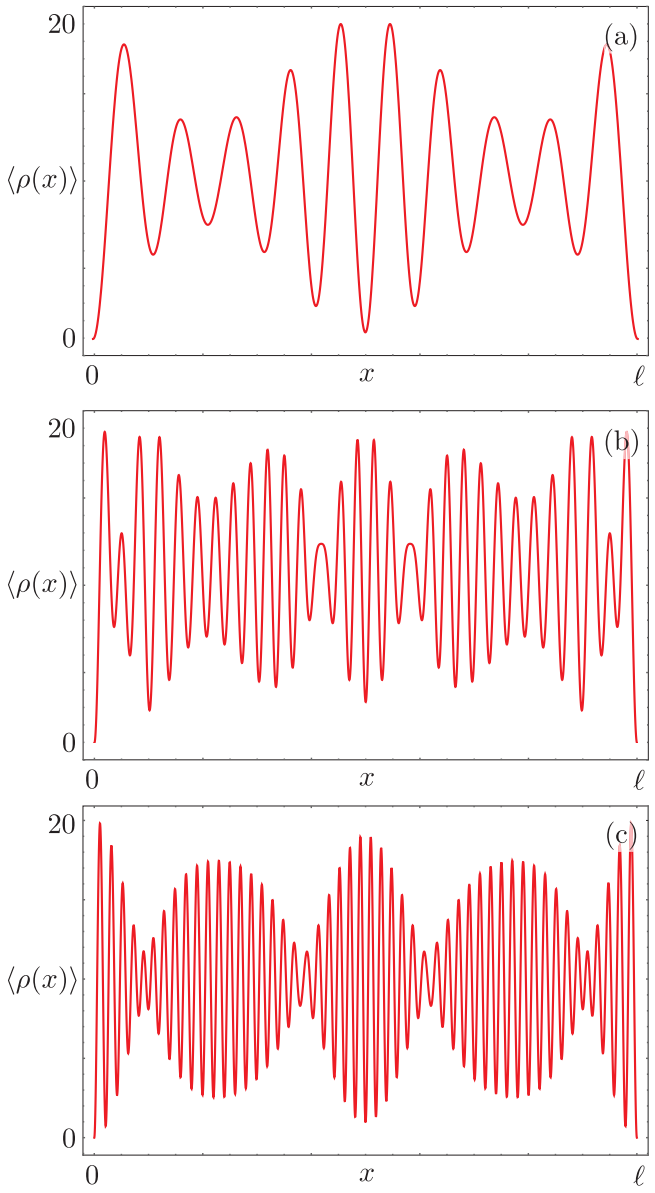

FIG. 2. (Color online) Same as in Fig. 1 but for $N_0 = 10$. All other parameters as in Fig. 1.

We close this section observing that the mechanism producing oscillations at wave vector $4(2n+1)k_F$ is intrinsic to the fractional helical liquid phase and independent of the boundary conditions. Therefore, a similar effect could be observed, for instance, in an infinite quantum wire in the presence of an impurity. The latter, breaking the translational invariance, would pin the density and allows for the predicted oscillations to be observed around the location of the impurity. Still, in actual implementations, quantum wires not adiabatically connected to external leads can behave as quantum dots, so that the setup chosen in the paper is of actual relevance in condensed matter.

B. Discussion

We comment here on the observability and stability of the predicted effect. Assuming InAs as a host material [33–35], tuning the resonance at $\nu = 1/3$ for a dot with $N_0 = 10$ electrons, one requires a length [48] $\ell \approx 7.5$ μm, while $\ell \approx 4.5$ μm is required for $N_0 = 6$—see Eq. (12). As put forward by several authors, density oscillations in a quantum dot can be probed by scanning a charged AFM tip along the wire while performing a linear transport experiment with lateral source and drain contacts [27,28,32,49,50]. The tip induces a chemical potential shift proportional to the dot density and a modulation of the conductance that is connected to the density oscillations [27,28,49,50]. The lateral resolution can be approximately estimated in the range of [28,50] $\approx$50 nm while the average wavelength of the density oscillations is $\approx$250 nm. Thus, such an experiment may detect the N_p peaks of the density oscillations.

The terms $V^{(n)}_{\mathrm{Z},7}(x)$ and $V^{(n+1)}_{\mathrm{Z},8}(x)$ can become relevant as long as their wavelength $\lambda = 2\pi q_7^{(n)} = 2\pi q_8^{(n+1)}$ is larger than the dot length ℓ, or equivalently

$$|\gamma_n k_{\mathrm{F}} - k_{\mathrm{SO}}| \leqslant \frac{2\pi}{\ell}. \tag{52}$$

Thus, the number of electrons in the dot and its length must be calibrated in order to satisfy the above condition. Note that Eq. (52) may allow for some flexibility for the resonance with $\nu = 1/3$: supposing, for instance, that $\gamma_1 k_{\mathrm{F}} - k_{\mathrm{SO}} = 0$ for N_0 dot electrons, one finds that the condition in Eq. (52) is still satisfied for $N_0 \pm 1$ electrons in the dot. This fact does not hold, however, for resonances with $n \geqslant 2$, for which the tuning of dot parameters is more critical.

The arguments developed in this paper rely on the infinite mass approximation for the sine-Gordon model, when the gap becomes the largest energy scale. Finite-size effects limit the flow of the renormalization-group equations. Therefore, the relevance of the terms $V^{(n)}_{\mathrm{Z},7}(x)$ and $V^{(n+1)}_{\mathrm{Z},8}(x)$ will depend strongly on the bare values of their coupling [18]. The latter, being proportional to the applied magnetic field, should be controllable in experiments [51].

In particular, increasing the magnetic field results in an increase of the coupling Δ. Clearly, a large magnetic field would also break the helicity of the system, creating a spin-polarized electron liquid. However, a lower bound for the magnetic field exists. This stems from the requirement that the Fermi energy of the given resonance lies between the bottom of the lower subband and the bottom of the main gap. This is satisfied for

$$B < \frac{\hbar^2 k_{\mathrm{SO}}^2}{g^* \mu_B m^*} \frac{2n}{2n+1}. \tag{53}$$

Renormalization-group arguments provide an upper threshold value on the Luttinger parameter $g_{\mathrm{c}} = 3/\gamma_n^2$ in order for a given resonance to be relevant. Estimating the actual strength of electron interactions is, however, beyond the scope of the model. More insight may be drawn from microscopical approaches such as the Hubbard model. This would not only allow us to confirm the predictions made here concerning the fixed point of the theory, but also in principle to observe the transition toward crystallization. In a recent paper [21], it was shown that for $V^{(n)}_{\mathrm{Z},7/8}$ to be relevant at $n \geqslant 1$, on-site repulsion (however strong) is not sufficient in the Hubbard model [42]. This seems to imply that a nonzero range interaction

is needed to observe the predicted effects. Indeed, although the bare Hamiltonian of the dot in Eq. (2) includes only zero-range interactions, the correction terms $\rho_W(x)$ and $\rho_Z(x)$ essentially capture the effects of such long-range interactions. So far, no clear experimental observation of a fractional helical liquid exists. One possible way to obtain strong interactions in condensed matter could be to minimize screening by suspending the nanowire acting as a dot—a technique that has been proven successful, e.g., for obtaining Wigner molecules in a carbon nanotube [52,53]. Also, a possible implementation could be speculated in cold-atoms systems. A one-dimensional Rashba wire subject to a perpendicular magnetic field could be simulated taking advantage of neutral cold atoms trapped in optical lattices. As discussed by Mancini *et al.* in Ref. [36] for alkaline-earth-like atoms, the joint action of the magnetic field with the Rashba spin-orbit coupling can be simulated using proper Raman transitions between different nuclear spin states. Cold-atoms realizations of our model may allow the observation of the fractional phase if one uses Rydberg atoms where longer-range interaction terms can be obtained [37].

When interactions are not strong enough, the mass of the sine-Gordon sector does not flow to very large values, and additional contributions to the density, which are negligible in the regime treated here, may compete or indeed become relevant. In particular, we can expect that with lowering interactions, a "shallower" oscillation with $(2n+1)N_0/2$ peaks, analogous to the conventional *Friedel oscillations*, may appear in the density. For even lower interactions, the standard Wigner and Friedel oscillations, with N_0 and $N_0/2$ peaks, respectively, are expected to set in.

V. CONCLUSIONS

We have studied the density oscillations of a quantum dot created in a spin-orbit coupled quantum wire in the presence of a magnetic field and strong repulsive electron interactions. When the density is tuned at fractional fillings $\nu = k_F/k_{SO} = 1/(2n+1)$, for sufficiently strong interactions a fractional gapped phase develops, for which we have shown that the density oscillates at the peculiar wave vector $4(2n+1)k_F$ and exhibits $(2n+1)N_0$ peaks for N_0 electrons in the dot. We believe that such peculiar density oscillations can be detected in linear transport experiments on state-of-the-art samples, probing the dot with a charged AFM tip [27,32].

ACKNOWLEDGMENTS

The authors wish to thank R. Fazio and N. Traverso Ziani for useful discussions. The financial support of MIUR-FIRB2012 under Grant No. RBFR1236VV and MIUR-PRIN under Project No. 2010LLKJBX is gratefully acknowledged.

APPENDIX: CORRECTIONS TO THE DENSITY

In this Appendix, we will evaluate the corrections to the long-wave density induced by nonresonating interaction terms $V_j^{(m)}(x)$—see Eq. (11). As we will show, such corrections oscillate with the same wave vector and are enveloped by the same slowly varying terms as the quantum average of the density correction terms $\rho_{Z,j}^{(m)}(x)$—see Eq. (27)—evaluated in Sec. III. A similar argument holds for umklapp terms [44], which generate the Wigner correction terms in Eq. (25). This identification motivates the approach proposed in the main text, namely to capture the leading corrections induced by nonresonating interaction terms by introducing corrections to the particle density operators within the framework of the sole Hamiltonian $H = h_0 + h_M$.

The starting point is the decoupled Hamiltonian $H \approx h_0 + h_M$—see Eqs. (15) and (16)—in the large mass limit when the field $\eta_+(x)$ is pinned to the minima of the cosine term in h_M. Due to open boundary conditions, the field $\eta_-(x)$ must satisfy the relations $\eta_-(-x) = -\eta_-(x)$ and $\eta_-(x+2\ell) = \eta_-(x)$. The massless sector is diagonalized by the bosonic fields

$$\eta_-(x) = i\sqrt{g_\eta}\sum_{n>0}\frac{e^{-\alpha\frac{\pi n}{2\ell}}}{\sqrt{n}}\sin\left(\frac{\pi n x}{\ell}\right)(b_n^\dagger - b_n), \quad \text{(A1)}$$

$$\chi_-(x) = \frac{1}{\sqrt{g_\eta}}\sum_{n>0}\frac{e^{-\alpha\frac{\pi n}{2\ell}}}{\sqrt{n}}\cos\left(\frac{\pi n x}{\ell}\right)(b_n^\dagger + b_n), \quad \text{(A2)}$$

satisfying $[\eta_-(x), \partial_{x'}\chi_-(x')] = i\pi\delta(x-x')$.

We will develop our argument for the terms $\propto \int_0^\ell dy\, V_j^{(m)}(y)$, the procedure for the umklapp term originating in the Wigner oscillations being the same. The perturbation we consider is

$$\begin{aligned}\delta h_j^{(m)} &= \frac{1}{2\pi}\int_0^\ell dy\, V_j^{(m)}(y)\\ &= \frac{\Delta_j^{(m)}}{2\pi}\int_0^\ell dy\cos\left[2q_j^{(m)}(y) - \sqrt{2}O_j^{(m)}(y)\right], \quad \text{(A3)}\end{aligned}$$

with $q_j^{(m)}$ and $O_j^{(m)}(y)$ given in Table I. We consider the lowest-order correction to the long-wave density of the system $\rho_{LW}(x)$,

$$\begin{aligned}\rho_{LW}(x) &= \frac{N_0}{\ell} + \frac{1}{\pi}\partial_x\phi_\rho(x)\\ &\equiv \frac{N_0}{\ell} + \frac{1}{\pi\sqrt{2}}\partial_x\left[\frac{1}{\sqrt{\gamma_n}}\eta_-(x) - f(x)\right]. \quad \text{(A4)}\end{aligned}$$

If we denote the ground state of the unperturbed system by $|\mathbf{0}\rangle$ and a generic unperturbed excited state by $|\boldsymbol{\mathcal{E}}\rangle$, with energy $E_{\mathbf{0}}$ and $E_{\boldsymbol{\mathcal{E}}}$, respectively, to lowest order in λ the new ground state is

$$\left|\Xi_j^{(m)}\right\rangle = |\mathbf{0}\rangle + \sum_{\boldsymbol{\mathcal{E}}}\frac{\langle\boldsymbol{\mathcal{E}}|\delta h_j^{(m)}|\mathbf{0}\rangle}{E_{\mathbf{0}} - E_{\boldsymbol{\mathcal{E}}}}|\boldsymbol{\mathcal{E}}\rangle. \quad \text{(A5)}$$

The first-order correction to the average of the long-wave density on the ground state is thus given by

$$\left\langle\delta\rho_{LW,j}^{(m)}(x)\right\rangle = \sum_{\boldsymbol{\mathcal{E}}}\frac{\langle\boldsymbol{\mathcal{E}}|\delta h_j^{(m)}|\mathbf{0}\rangle}{E_{\mathbf{0}} - E_{\boldsymbol{\mathcal{E}}}}\langle\mathbf{0}|\rho_{LW}(x)|\boldsymbol{\mathcal{E}}\rangle + \text{c.c.} \quad \text{(A6)}$$

We have $|\boldsymbol{\mathcal{E}}\rangle = |\omega,\Omega_p\rangle$ and $|\mathbf{0}\rangle = |0,\Omega_q\rangle$, where ω labels the excited states of h_0, and Ω_q denotes the eigenstate of h_M with $\eta_+(x)$ pinned in the qth minima of the cosine term. Since we consider the very large mass limit, the lowest-lying excitations are due to the massless sector only, while the massive mode remains fully gapped: $E_{\mathbf{0}} - E_{\boldsymbol{\mathcal{E}}} = E_0 - E_\omega$, where the

energies on the right-hand side refer to the unperturbed ground state and excited states of h_0. To evaluate the correction to the average of the long-wave density in Eq. (A6), it is necessary to express the operator $O_j^{(m)}(y)$ in Eq. (A3) in terms of the fields $\eta_\pm(y)$ and $\chi_\pm(y)$ through the canonical transformation introduced in Eq. (14). Then, Eq. (A6) becomes

$$\left\langle \delta\rho^{(m)}_{\mathrm{LW},j}(x)\right\rangle = \frac{\Delta_j^{(m)}}{2\pi^2\sqrt{2\gamma_n}}\int_0^\ell dy \sum_{\xi=\pm} C^{(m)}_{\xi,j}(x,y) \times D^{(m)}_{\xi,j}(y) e^{i\xi Q_j^{(m)}(y)} + \text{c.c.}, \tag{A7}$$

where

$$Q_j^{\prime(m)}(y) = 2q_j^{(m)} y + \left[c_j^{(m)} - \alpha^{(m)}_{-,j}\beta^{(m)}_{+,j}\right] f(y) \tag{A8}$$

and

$$C^{(m)}_{\xi,j}(x,y) = \sum_\omega \frac{1}{E_0 - E_\omega}\langle\omega| e^{i\xi\alpha^{(m)}_{-,j}\eta_-(y)+i\xi\beta^{(m)}_{-,j}\chi_-(y)}|0\rangle \times \langle 0|\partial_x\eta_-(x)|\omega\rangle, \tag{A9}$$

$$D^{(m)}_{\xi,j}(y) = \left\langle e^{i\xi\alpha^{(m)}_{+,j}\eta_+(y)+i\xi\beta^{(m)}_{+,j}\chi_+(y)}\right\rangle_\Omega. \tag{A10}$$

Here, we have introduced the scalar coefficients $c_j^{(m)}$, $\alpha^{(m)}_{\pm,j}$, and $\beta^{(m)}_{\pm,j}$, which stem from the canonical transformation. Note that Eq. (A8) also includes the effects of commutators between fields. Finally, the notation $\langle\cdots\rangle_\Omega$ in Eq. (A10) represents the average over the equivalent states $|\Omega_q\rangle$—see Eqs. (33) and (34) for details. To evaluate $C^{(m)}_{\xi,j}(x,y)$, one can use the explicit form of the fields given in Eqs. (A1) and (A2). We obtain

$$C^{(m)}_{\xi,j}(x,y) = \frac{\xi\sqrt{g_\eta}}{v_\eta}[K(y)]^{\frac{g_\eta\left[\alpha^{(m)}_{-,j}\right]^2}{4}}[G(y)]^{\frac{\left[\beta^{(m)}_{-,j}\right]^2}{4g_\eta}} \times \sum_{k>0} A^{(m)}_{k,j}(y)\cos\left(\frac{\pi kx}{\ell}\right), \tag{A11}$$

where $K(y)$ and $G(y)$ are given in Eqs. (45) and (47), and

$$A^{(m)}_{k,j}(y) = \frac{e^{-\alpha\frac{\pi k}{\ell}}}{k}\left[\frac{\beta^{(m)}_{-,j}}{\sqrt{g_\eta}}\cos\left(\frac{\pi ky}{\ell}\right) + i\alpha^{(m)}_{-,j}\sqrt{g_\eta}\sin\left(\frac{\pi ky}{\ell}\right)\right].$$

The evaluation of $D^{(m)}_{\xi,j}(y)$ can be performed following the same procedure outlined in Sec. III—see Eqs. (33) and (34)—so we quote here the result only:

$$D^{(m)}_{\pm,j}(y) = (-1)^l\delta_{\alpha^{(m)}_{+,j},2l}[E(y)]^{\frac{\left[\beta^{(m)}_{+,j}\right]^2}{2}} \equiv D_j^{(m)}(y), \tag{A12}$$

with $l\in\mathbb{Z}$ and $E(y)$ a vanishing function in the infinite mass limit—see Eq. (36). Coming back to Eq. (A7), we have

$$\left\langle \delta\rho^{(m)}_{\mathrm{LW},j}(x)\right\rangle = \frac{g_\eta\alpha^{(m)}_{-,j}\Delta_j^{(m)}}{\pi v_\eta\sqrt{2\gamma_n}}\int_0^\ell dy\, D_j^{(m)}(y)[K(y)]^{\frac{g_\eta\left[\alpha^{(m)}_{-,j}\right]^2}{4}} \times [G(y)]^{\frac{\left[\beta^{(m)}_{-,j}\right]^2}{4g_\eta}}\sin\left[Q_j^{\prime(m)}(y)\right]\left[\Theta(y-x) - \frac{y}{L}\right], \tag{A13}$$

where $\Theta(y-x)$ is the Heaviside function and we have used the approximation $\sum_{k>0} e^{-\alpha\frac{\pi k}{\ell}}\sin(\pi ky/\ell)\cos(\pi kx/\ell)/k \approx \pi/2[\Theta(y-x) - y/L]$. At this point, it is helpful to note that the functions $D_j^{(m)}(y)$, $K(y)$, $G(y)$, and $f(y)$ are slowly varying on the scale of ℓ. Thus, using integration by parts, one arrives at the final result,

$$\left\langle \delta\rho^{(m)}_{\mathrm{LW},j}(x)\right\rangle = \frac{g_\eta\alpha^{(m)}_{-,j}\Delta_j^{(m)}}{\pi v_\eta\sqrt{2\gamma_n}}D_j^{(m)}(x)[K(y)]^{\frac{g_\eta\left[\alpha^{(m)}_{-,j}\right]^2}{4}} \times [G(y)]^{\frac{\left[\beta^{(m)}_{-,j}\right]^2}{4g_\eta}}\frac{\cos\left[Q_j^{\prime(m)}(x)\right]}{q_j^{(m)}}. \tag{A14}$$

Therefore, to lowest order, the perturbation $V_j^{(m)}$ generates a correction to the average long-wave density of the system oscillating with wave vector $q_j^{(m)}$ and enveloped by slowly varying functions. The result coincides with the average of the density correction terms introduced in Eq. (20)—see Eq. (50)—and motivates the approach followed in the main text.

[1] T. Meng and D. Loss, Phys. Rev. B **88**, 035437 (2013).
[2] P. Streda and P. Seba, Phys. Rev. Lett. **90**, 256601 (2003).
[3] Y. V. Pershin, J. A. Nesteroff, and V. Privman, Phys. Rev. B **69**, 121306 (2004).
[4] C. H. L. Quay, T. L. Hughes, J. A. Sulpizio, L. N. Pfeiffer, K. W. Baldwin, K. W. West, D. Goldhaber-Gordon, and R. de Picciotto, Nat. Phys. **6**, 336 (2010).
[5] T. Meng and D. Loss, Phys. Rev. B **87**, 235427 (2013).
[6] F. M. Gambetta, N. Traverso Ziani, S. Barbarino, F. Cavaliere, and M. Sassetti, Phys. Rev. B **91**, 235421 (2015).
[7] R. Li, L.-A. Wu, X. Hu, and J. Q. You, arXiv:1509.03402.
[8] J. Klinovaja and D. Loss, Phys. Rev. B **86**, 085408 (2012).
[9] D. E. Liu and A. Levchenko, Phys. Rev. B **88**, 155315 (2013).
[10] Q. Meng, T. L. Hughes, M. J. Gilbert, and S. Vishveshwara, Phys. Rev. B **86**, 155110 (2012).
[11] B. Braunecker, G. I. Japaridze, J. Klinovaja, and D. Loss, Phys. Rev. B **82**, 045127 (2010).
[12] T. Meng, J. Klinovaja, and D. Loss, Phys. Rev. B **89**, 205133 (2014).
[13] C. L. Kane, R. Mukhopadhyay, and T. C. Lubensky, Phys. Rev. Lett. **88**, 036401 (2002).
[14] J. C. Y. Teo and C. L. Kane, Phys. Rev. B **89**, 085101 (2014).
[15] J. Voit, Rep. Prog. Phys. **58**, 977 (1995).
[16] J. von Delft and H. Schoeller, Ann. Phys. **7**, 225 (1998).
[17] T. Giamarchi, *Quantum Physics in One Dimension* (Oxford Science, Oxford, UK, 2004).
[18] Y. Oreg, E. Sela, and A. Stern, Phys. Rev. B **89**, 115402 (2014).
[19] T. Meng, L. Fritz, D. Schuricht, and D. Loss, Phys. Rev. B **89**, 045111 (2014).

[20] E. Cornfeld, I. Neder, and E. Sela, Phys. Rev. B **91**, 115427 (2015).
[21] E. Cornfeld and E. Sela, Phys. Rev. B **92**, 115446 (2015).
[22] G. Giuliani and G. Vignale, *Quantum Theory of the Electron Liquid* (Cambridge University Press, Cambridge, UK, 2005).
[23] M. Fabrizio and A. O. Gogolin, Phys. Rev. B **51**, 17827 (1995).
[24] K. Jauregui, W. Haüsler, and B. Kramer, Europhys. Lett. **24**, 581 (1993).
[25] W. Haüsler and B. Kramer, Phys. Rev. B **47**, 16353 (1993).
[26] A. Secchi and M. Rontani, Phys. Rev. B **80**, 041404 (2009).
[27] J. Qian, B. I. Halperin, and E. J. Heller, Phys. Rev. B **81**, 125323 (2010).
[28] N. Traverso Ziani, F. Cavaliere, and M. Sassetti, Phys. Rev. B **86**, 125451 (2012).
[29] In principle, both Friedel and Wigner oscillations display a series of higher harmonics at integer multiples of their respective wave vectors; see Ref. [31]. For standard wires, however, the most relevant contribution is due to the fundamental mode.
[30] F. M. Gambetta, N. Traverso Ziani, F. Cavaliere, and M. Sassetti, Europhys. Lett. **107**, 47010 (2014).
[31] I. Safi and H. J. Schulz, Phys. Rev. B **59**, 3040 (1999).
[32] D. Mantelli, F. Cavaliere, and M. Sassetti, J. Phys.: Condens. Matter **24**, 432202 (2012).
[33] Y. Sidor, B. Partoens, F. M. Peeters, T. Ben, A. Ponce, D. L. Sales, S. I. Molina, D. Fuster, L. González, and Y. González, Phys. Rev. B **75**, 125120 (2007).
[34] S. Csonka, L. Hofstetter, F. Freitag, S. Oberholzer, C. Schönenberger, T. S. Jespersen, M. Aagesen, and J. Nygard, Nano Lett. **8**, 3932 (2008).
[35] D. Liang and X. P. A. Gao, Nano Lett. **12**, 3263 (2012).
[36] M. Mancini *et al.*, Science **349**, 1510 (2015).
[37] P. Schauß *et al.*, Nature (London) **491**, 87 (2012).
[38] Y. Gindikin and V. A. Sablikov, Phys. Rev. B **76**, 045122 (2007).
[39] In principle, more general terms of the form $U_n(x)V_j(x)U_{n'}(x)$ with $n \neq n'$ could be considered. The results in the regime considered in this paper, however, are not affected by such terms.
[40] From Table I it follows that when $n = 0$ one has $q_3^{(0)} = q_7^{(0)}$, $q_4^{(0)} = q_8^{(0)}$ and $O_3^{(0)}(x) = O_7^{(0)}(x)$, $O_4^{(0)}(x) = O_8^{(0)}(x)$. Therefore, the pairs of terms $V_3^{(0)}(x)$, $V_7^{(0)}(x)$ and $V_4^{(0)}(x)$, $V_8^{(0)}(x)$ describe the same process. In particular, as we will show at the end of this section, the term $V_3^{(0)}(x) \equiv V_7^{(0)}(x)$ is responsible for opening the main gap of the theory. Thus, since in the rest of the paper we will focus on the fractional gaps occurring for $n \geqslant 1$, this detail is not important for our discussion.
[41] Even-denominator resonances, generated by interaction terms with comparable amplitude $V_5^{(n)}(x)$ and $V_6^{(n)}(x)$, give rise to a self-dual sine-Gordon problem due to the noncommutativity of $O_5^{(n)}(x)$ and $O_6^{(n)}(x)$. Such a problem is much harder to treat than a standard sine-Gordon problem—see, e.g., P. Lecheminant, A. O. Gogolin, and A. A. Nersesyan, Nucl. Phys. B **639**, 502 (2002)—and few general results are known. We defer the analysis of these terms to possible future works and focus on the odd-denominator states whose physics is more immediate.
[42] H. J. Schulz, Phys. Rev. Lett. **64**, 2831 (1990).
[43] H. J. Schulz, Phys. Rev. Lett. **71**, 1864 (1993).
[44] S. A. Söffing, M. Bortz, I. Schneider, A. Struck, M. Fleischhauer, and S. Eggert, Phys. Rev. B **79**, 195114 (2009).
[45] F. D. M. Haldane, J. Phys. C **14**, 2585 (1981).
[46] D. L. Maslov and M. Stone, Phys. Rev. B **52**, R5539(R) (1995).
[47] N. Traverso Ziani, F. Crépin, and B. Trauzettel, Phys. Rev. Lett. **115**, 206402 (2015).
[48] For this estimate, following Ref. [34] we have assumed $g_{\rm SO} = 2 \times 10^{-11}$eV m and $m^* = 0.023m_{\rm e}$, with $m_{\rm e} = 9.1 \times 10^{-31}$K g the bare electron mass.
[49] A. A. Zhukov, Ch. Volk, A. Winden, H. Hardtdegen, and Th. Schäpers, JETP Lett. **96**, 109 (2012).
[50] A. A. Zhukov, Ch. Volk, A. Winden, H. Hardtdegen, and Th. Schäpers, JETP **116**, 138 (2013).
[51] Note that, for the case of InAs, a large effective Landé g-factor is reported [34], $g^* \approx 5$.
[52] S. Pecker *et al.*, Nat. Phys. **9**, 576 (2013).
[53] N. Traverso Ziani, F. Cavaliere, and M. Sassetti, J. Phys.: Condens. Matter **25**, 342201 (2013).